The reverse reaction takes place at room temperature, giving brown-red $SCl_3[OsCl_6]$ as a very hydrolysis-sensitive crystal powder. Anal. Calcd: Cl, 58.94; S, 5.92. Found: Cl, 58.33, S, 5.43.

The IR spectrum of $SCl_3[OsCl_6]$ exhibits strong absorption bands due to the $SCl_3^+$ ion ($cm^{-1}$): 494 vs, $\nu_{as}$ $SCl_3$ (E); 469 s, $\nu_s$ $SCl_3$ ($A_1$); 265 s, $\delta$ $SCl_3$ ($A_1$). These values are comparable, although somewhat lower, with those in other $SCl_3^+$ compounds.[11] The $F_{1u}$ stretching vibration of the $OsCl_6^-$ ion is observed as a strong band at 313 $cm^{-1}$. This value is lower than in other $OsCl_6^-$ compounds, an effect that probably has to do with the electrostatic interaction between ions, as decreasing cation size goes parallel with decreasing frequency (cf. $AsPh_4[OsCl_6]$ (337 $cm^{-1}$),[3] $PPh_4[OsCl_6]$ (338, 330 sh $cm^{-1}$),[1] $NEt_4[OsCl_6]$ (325 $cm^{-1}$).[4]

**Registry No.** $PPh_4[OsCl_6]$, 86365-50-6; $SCl_3[OsCl_6]$, 91002-45-8.

Fachbereich Chemie
Universität Marburg
D-3550 Marburg, West Germany

**Kurt Dehnicke***
**Ulrich Müller**
**Rainer Weber**

*Received April 30, 1984*

(11) Weidlein, J.; Müller, U.; Dehnicke, K. "Schwingungsfrequenzen I"; G. Thieme Verlag: Stuttgart, New York, 1981.

# Articles

Contribution from the Department of Chemistry and Biochemistry, Utah State University, Logan, Utah 84322, and Department of Chemistry, University of Arizona, Tucson, Arizona 85721

## Molybdenum(VI)-Dioxo Complexes with Sterically Bulky Ligands

P. SUBRAMANIAN,[1a] J. T. SPENCE,*[1a] R. ORTEGA,[1b] and J. H. ENEMARK[1b]

*Received March 13, 1984*

New molybdenum(VI)-dioxo complexes with a number of ligands having sterically bulky substituents have been synthesized. One-electron coulometric reduction of $MoO_2LH_2$ complexes ($LH_4$ = *N,N'*-bis(2-hydroxy-3-*tert*-butylbenzyl)-1,2-diaminoethane (3-*t*-Bu-hbe$H_4$) and related ligands having 3-*tert*-butyl groups and *N,N'*-bis(2-ethyl-2-mercaptobutyl)-1,2-diaminoethane) in aprotic solvents gives stable Mo(V) monomers, while complexes without these ligand structures give Mo(V) oxo-bridged dimers. The X-ray structure of $MoO_2$(3-*t*-Bu-hbe$H_2$) indicates the molecule has effective $C_2$ symmetry and suggests oxo-bridged dimer formation upon reduction is prevented by the 3-*tert*-butyl groups by steric hindrance. The room-temperature EPR spectra of the Mo(V) complexes exhibit coupling of 0.21-0.26 mT to two $^{14}N$ nuclei, indicating the ligands likely have deprotonated amino groups. Chemical reduction of $MoO_2LH_2$ gives $MoOLH_2$ complexes which, upon one-electron coulometric oxidation, give Mo(V) complexes without $^{14}N$ coupling to the Mo(V) EPR signal and with EPR parameters different from those of the complexes obtained by one-electron reduction of $MoO_2LH_2$.

### Introduction

Molybdenum is an essential component of a number of enzymes that catalyze two-electron redox processes.[2,3] The molybdenum centers are thought to cycle between the VI, V, and IV oxidation states during catalysis, with the distribution of electrons between the molybdenum and other redox centers of the enzymes governed by their relative reduction potentials.[2,4] The results of recent EXAFS[5] and EPR[6] investigations of sulfite oxidase and assimilatory nitrate reductase indicate the presence of two oxo ligands, two or three thiolate ligands, and, possibly, additional nitrogen, oxygen, or thioether ligands of molybdenum in the oxidized (Mo(VI)) state. Upon reduction (Mo(V/IV)), one oxo is lost; EPR evidence suggests it is converted to an $OH^-$ ligand.[5,6]

A large number of Mo(VI)-dioxo complexes are known, some of which have been proposed as models for the molybdenum centers of these enzymes.[7-11] Upon one-electron reduction, however, most Mo(VI)-dioxo complexes give EPR-silent, Mo(V) oxo-bridged dimers:[12]

$$H_2O + 2Mo^{VI}O_2L \xrightarrow{2e^-} Mo_2O_3L_2 + 2OH^-$$

In our search for more satisfactory models, we have synthesized a number of new Mo(VI)-dioxo complexes with sterically bulky ligands that inhibit the close approach of two Mo(V)-oxo centers required for oxo-bridge formation. The syntheses and properties of these complexes, the X-ray structure of one of the complexes, and the ability of various ligand structures to inhibit dimerization upon electrochemical reduction of the complexes are reported here.

### Results

Complexes with bidentate NS, tridentate NOS, and tetradentate $N_2O_2$ and $N_2S_2$ ligands with five basic structures have been synthesized (Table I). In all cases where R ≠ H, examination of stereo models indicates some degree of steric interaction between ligands in Mo(V) oxo-bridged dimers is to be expected.

**Electrochemistry.** All complexes exhibit an irreversible reduction peak in their cyclic voltammograms at a negative potential (−0.99 to −1.65 V vs. SCE; Table II). This peak

(1) (a) Utah State University. (b) University of Arizona.
(2) Bray, R. C. *Adv. Enzymol. Relat. Areas Mol. Biol.* **1980**, *51*, 107.
(3) Hewitt, E. J.; Notton, B. A. In "Molybdenum and Molybdenum Containing Enzymes"; Coughlan, M., Ed.; Pergamon Press: New York, 1980; p 273.
(4) Olson, J. S.; Ballou, D. P.; Palmer, G.; Massey, V. *J. Biol. Chem.* **1974**, *249*, 4363.
(5) Cramer, S. P.; Wahl, R.; Rajagopalan, K. V. *J. Am. Chem. Soc.* **1981**, *103*, 7721. Cramer, S. P.; Solomonson, L. S.; Adams, M. W. W.; Mortenson, L. E. *Ibid.* **1984**, *106*, 1467.
(6) Gutteridge, S.; Bray, R. C. *Biochemistry* **1982**, *21*, 5992. Bray, R. C.; Gutteridge, S.; Lamy, M. T.; Wilkinson, T. *Biochem. J.* **1983**, *211*, 227.
(7) Stiefel, E. I. *Prog. Inorg. Chem.* **1977**, *22*, 1.
(8) Stiefel, E. I. Reference 3, p 41. Spence, J. T. *Ibid.*, p 99. Stiefel, E. I. *Chem. Uses Molybdenum, Proc. Int. Conf.* **1982**, *4*, 56.
(9) Spence, J. T. *Coord. Chem. Rev.* **1983**, *48*, 59.
(10) Rajan, O. A.; Spence, J. T.; Leman, C.; Minelli, M.; Sato, M.; Enemark, J. H.; Kroneck, P. M. H.; Sulger, K. *Inorg. Chem.* **1983**, *22*, 3065.
(11) Spence, J. T.; Minelli, M.; Kroneck, P. *J. Am. Chem. Soc.* **1980**, *102*, 4538.
(12) Chen, G. J.-J.; McDonald, J. W.; Newton, W. E. *Inorg. Chem.* **1976**, *15*, 2612.

0020-1669/84/1323-2564$01.50/0 

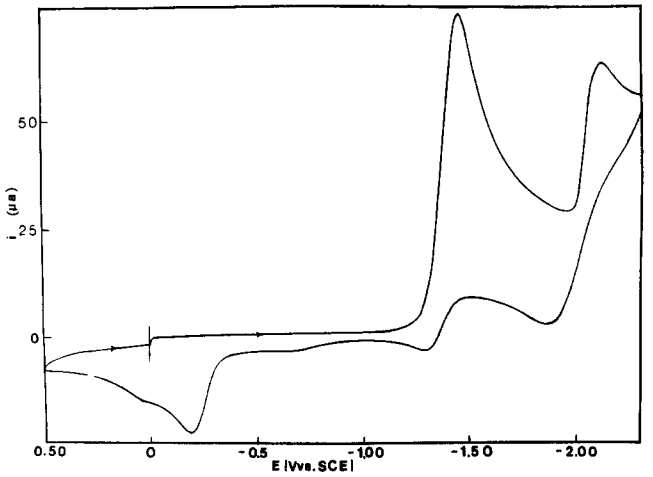


**Figure 1.** Cyclic voltammogram of $MoO_2$(3-*t*-Bu-hbeH$_2$) (**15**) (3.20 × $10^{-3}$ M) (0.10 M [*n*-$Bu_4N$][$BF_4$] in DMF; scan rate 0.100 V $s^{-1}$).

is coupled to an oxidation peak at a considerably more positive potential (Figure 1). In some cases (complexes **15–20**) this reduction peak shows quasi-reversible character as the scan rate is increased, with accompanying decrease in the height of the oxidation peak at more positive potential; as the rate is increased, however, $\Delta E_p$ for the quasi-reversible cathodic and anodic peaks increases. A second reduction peak at a more negative potential is also observed with certain complexes (Table II; Figure 1).

Coulometric reduction at a potential just negative of the first reduction peak was carried out for all complexes. For **1–3**, reduction ceases after addition of 0.3–0.6 electron/molecule, the solution becomes cloudy, and the CV shows loss of the Mo(VI)–dioxo complex and a number of small peaks, indicating decomposition. Such behavior has been observed by others for similar complexes.[13] For **4–18** and **20**, reduction ceases after addition of ~1.00 electron/molecule and the CV shows complete reduction of the Mo(VI)–dioxo complex; the oxidation peak at more positive potential remains, and a complete scan exhibits the original coupled reduction peak. For complex **19**, reduction consumes ~2 electrons/molecule, apparently proceeding to the Mo(IV) state. Reduction of **21** also appears to consume approximately 2 electrons/molecule, but the current does not return completely to its background level, making determination of this value uncertain. The CV of the reduced solution of **21** exhibits no major oxidation or reduction peaks, and the electronic spectrum shows no absorbance above ~300 nm; apparently this complex decomposes upon complete reduction. Similar results were observed with the known complex $MoO_2$(mpeH$_2$) (mpeH$_4$ = *N*,*N*′-bis(2-mercapto-2-methylpropyl)-1,2-diaminoethane).[14]

**EPR.** EPR spectra were recorded at both room temperature and 77 K for solutions of the one-electron-reduced products. Quantitative spin concentrations of less than 5% of total Mo were observed for **4–14** and **20**, indicating EPR-silent dimers are the major product of reduction. For **19**, the spin concentration of Mo(V) was 1% after addition of 1 electron/molecule. For complexes (**15–18**) with tetradentate $N_2O_2$ ligands and $R_1$ = *t*-Bu, spin concentrations of 100 ± 10% were found. Furthermore, these Mo(V) monomers were observed to be stable upon the addition of 2 equiv of $H_2O$ or [*n*-$Bu_4N$]OH. Upon addition of 1 electron/molecule, **21** was found to have a spin concentration of 50 ± 10%; the CV of the reduced solution indicated the reduction peak at −1.54 V had been reduced to approximately 25% of its original height,

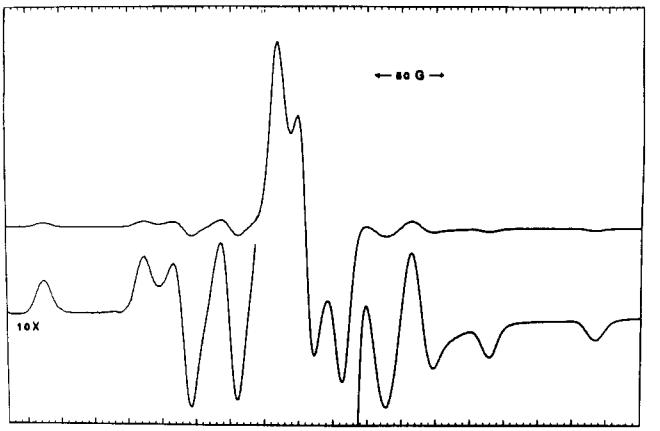


**Figure 2.** EPR spectrum of [MoO(3-*t*-Bu-hbe)]$^-$ (**15**$^-$) (5.00 × $10^{-4}$ M) (0.10 M [(*n*-$Bu)_4N$][$BF_4$] in DMF; 77 K).

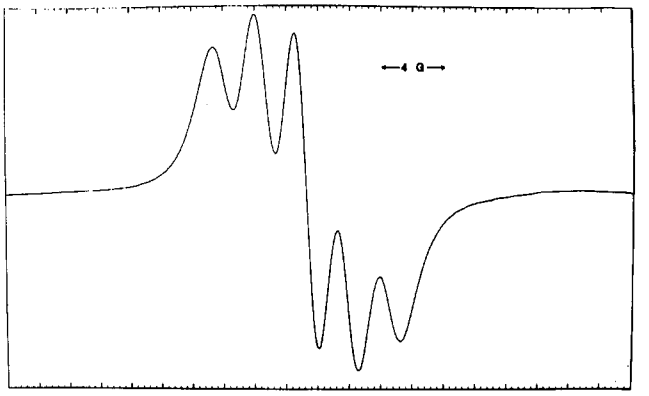


**Figure 3.** EPR spectrum of [MoO(3-*t*-Bu-hbe)]$^-$ (**15**$^-$) (5.00 × $10^{-4}$ M) (0.10 M [(*n*-$Bu)_4N$][$BF_4$] in DMF; room temperature).

and a new peak at −1.62 V was observed. Again, similar results were obtained with the known complex $MoO_2$(mpeH$_2$),[14] which also gave a Mo(V) concentration of 50 ± 10% upon one-electron reduction.

The frozen EPR spectra are rhombic, except for **21** (Figure 2; Table III). Surprisingly, the room-temperature EPR spectra of **15–18**, **21**, and [MoO(mpe)]$^-$ exhibit superhyperfine splitting of two $^{14}N$ nuclei: for complexes **15** and **16** ($R_3$ = $-(CH_2)_2-$) two equivalent $^{14}N$ with five lines (Figure 3); for complexes **17** and **18** ($R_3$ = *cis*-1,2-cyclohexanediyl and $-CH_2C(CH_3)_2-$) two nonequivalent $^{14}N$ with seven lines. For **21** and [MoO(mpe)]$^-$, splitting by two equivalent $^{14}N$ nuclei is also observed. Upon treatment with 2 equiv of the strong acid $CF_3SO_3H$, the Mo(V) products of **15** and **21** gave solutions with EPR (no $^{14}N$ coupling) and electronic spectra identical with the one-electron-oxidized products of the corresponding Mo(IV) complexes **22** and **23** described below.

Attempts to synthesize the Mo(V) complexes obtained by electrochemical reduction of Mo(VI)–dioxo complexes **15–18** and **21** in solution have been unsuccessful.

**X-ray Structure of $MoO_2$(3-*t*-Bu-hbeH$_2$).** A view of the structure of one of the two crystallographically independent $MoO_2LH_2$ molecules in the unit cell is shown in Figure 4. Pertinent interatomic distances for both molecules are summarized in Table VI. A least-squares analysis[15] on the molecular parameters of the two independent molecules showed that they are nearly identical. The maximum deviation from an ideal fit was 0.66 Å (C210 to C49), and the average deviation for all atoms was 0.25 Å. Each molecule has effective $C_2$ symmetry, and Table VI shows that the coordination symmetry of the *cis*-$MoO_4N_2$ core is nearly $C_{2v}$. Each mol-

(13) Stiefel, E. I., private communication.
(14) Taylor, R. D.; Street, J. P.; Minelli, M.; Spence, J. T. *Inorg. Chem.* **1978**, *17*, 3207.
(15) Yuen, P. S.; Nyberg, S. C. *J. Appl. Crystallogr.* **1979**, *12*, 258.

Table I. Complexes

| no. | | analyses,[a] % C | H | N | S | IR (Mo=O),[b] $cm^{-1}$ |
|---|---|---|---|---|---|---|
| | $MoO_2(R_1NHCH_2C(R_2)_2S)_2$ | | | | | |
| 1 | $R_1$ = Me, $R_2$ = Et | 40.15 (39.98) | 7.77 (7.67) | 6.74 (6.66) | 15.36 (15.25) | 884, 855 |
| 2 | $R_1 = R_2$ = Et | 42.64 (42.86) | 8.24 (8.04) | 6.14 (6.25) | 14.06 (14.29) | 882, 848 |
| 3 | $R_1$ = Et, $R_2$ = Me | 36.74 (36.74) | 7.01 (7.14) | 7.05 (7.14) | 16.09 (16.33) | 885, 852 |
| | 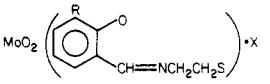 | | | | | |
| 4 | R = H, X = none (saet) | 35.06 (35.17) | 3.07 (2.93) | 4.32 (4.56) | 10.32 (10.42) | 920, 900, 890 |
| 5 | R = H, X = py (saet(py)) | 43.71 (43.52) | 3.72 (3.63) | 7.00 (7.25) | 8.03 (8.29) | 915, 845 |
| 6 | R = Me, X = py (3-Me-saet(py)) | 45.19 (45.00) | 4.10 (4.00) | 7.05 (7.00) | 7.81 (8.00) | 920, 892 |
| 7 | R = *i*-Pr, X = Im (3-*i*-Pr-saet(Im)) | 43.32 (43.17) | 4.61 (4.56) | 10.08 (10.07) | 7.51 (7.67) | 910, 880 |
| 8 | R = *t*-Bu, X = HMPA (3-*t*-Bu-saet(HMPA)) | 42.06 (42.07) | 6.62 (6.46) | 10.41 (10.33) | 5.75 (5.90) | 885, 914 |
| 9 | R = Ph, X = $Me_2SO$ (3-Ph-saet($Me_2SO$)) | 43.94 (45.84) | 4.39 (4.27) | 3.11 (3.15) | 13.13 (14.38) | 910, 890 |
| | 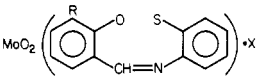 | | | | | |
| 10 | R = OMe, X = none (3-OMe-sma) | 43.81 (43.63) | 3.08 (2.86) | 3.61 (3.64) | 8.09 (8.31) | 915 |
| 11 | R = *i*-Pr, X = py (3-*i*-Pr-sma(py)) | 53.21 (52.94) | 4.47 (4.20) | 6.00 (5.88) | 6.57 (6.72) | 915, 890 |
| 12 | R = 3-*t*-Bu, X = py (3-*t*-Bu-sma(py)) | 53.92 (53.88) | 4.51 (4.49) | 5.74 (5.71) | 6.35 (6.53) | 920, 898 |
| 13 | R = Ph, X = py (3-Ph-sma(py)) | 56.47 (53.49) | 3.53 (4.08) | 5.49 (4.58) | 6.27 (6.82) | 914, 886 |
| | 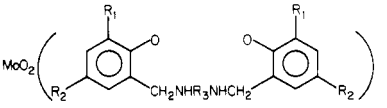 | | | | | |
| 14 | $R_1 = R_2$ = H, $R_3$ = -$(CH_2)_2$- ($hbeH_4$ ($Me_2SO$ adduct)) | 45.27 (45.37) | 4.95 (5.04) | 5.72 (5.88) | 6.03 (6.72) | 920, 880 |
| 15 | $R_1$ = *t*-Bu, $R_2$ = H, $R_3$ = -$(CH_2)_2$- (3-*t*-Bu-$hbeH_4$) | 56.47 (56.25) | 6.67 (6.49) | 5.49 (5.45) | | 924, 882 |
| 16 | $R_1 = R_2$ = *t*-Bu, $R_3$ = -$(CH_2)_2$- (3,5-di-*t*-Bu-$hbeH_4$) | 61.52 (61.72) | 7.94 (8.09) | 4.45 (4.50) | | 917, 906 |
| 17 | $R_1 = R_2$ = *t*-Bu, $R_3$ = 1,2-Cy(3,5-di-*t*-Bu-$hbcH_4$) | 63.86 (63.91) | 8.31 (8.28) | 3.98 (4.14) | | 922, 894 |
| 18 | $R_1 = R_2$ = *t*-Bu, $R_3$ = -$CH_2C(Me)_2$- (3,5-di-*t*-Bu-$hbmeH_4$) | 62.00 (62.77) | 8.39 (8.31) | 4.28 (4.31) | | 923, 903 |
| 19 | $R_1 = R_2$ = *t*-Bu, $R_3$ = -$(CH_2)_3$- (3,5-di-*t*-Bu-$hbpH_4$) | 62.01 (62.26) | 8.28 (8.18) | 4.41 (4.40) | | 911, 892 |
| 20 | $R_1$ = Ph, $R_2$ = H, $R_3$ = -$(CH_2)$- (3-Ph-$hbeH_4$) | 60.93 (61.09) | 4.88 (4.73) | 4.94 (5.09) | | 918, 880 |
| | $MoO_2(SC(R)_2CH_2NH(CH_2)_2NHCH_2C(R)_2S)$ | | | | | |
| 21 | R = Et ($mbeH_4$) | 40.34 (40.19) | 7.28 (7.18) | 6.69 (6.70) | 7.51 (7.66) | 895, 870 |
| | R = Me[c] ($mpeH_4$) | | | | | 893, 872 |
| | 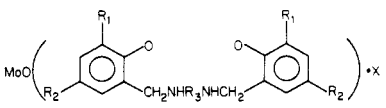 | | | | | |
| 22 | $R_1$ = *t*-Bu, $R_2$ = H, $R_3$ = -$(CH_2)_2$-, X = $CH_3OH$ (3-*t*-Buh$beH_4(CH_3OH)$) | 57.11 (57.03) | 6.96 (7.22) | 5.27 (5.32) | | 928 |
| | $MoO(SC(R)_2CH_2NH(CH_2)_2NHCH_2C(R)_2S)$ | | | | | |
| 23 | R = Et ($mbeH_4$) | 41.77 (41.79) | 7.44 (7.35) | 6.92 (6.86) | 7.68 (7.84) | 946 |
| | R = Me[d] ($mpeH_4$) | | | | | 950 |

[a] Calculated values in parentheses. [b] Nujol mulls. [c] Reference 14. [d] Reference 17.

Table II. Electrochemical Parameters

| complex | $E_c$,[a] V | $E_a$,[b] V | $n$[c] | $E_c'$,[e] V |
|---|---|---|---|---|
| $MoO_2(MeNCH_2CEt_2S)_2$[d] (1) | −1.65 | −0.77 | | |
| $MoO_2(EtNCH_2CEt_2S)_2$[d] (2) | −1.53 | −0.70 | | |
| $MoO_2(EtNCH_2CMe_2S)_2$[d] (3) | −1.40 | −0.75 | | |
| $MoO_2$(saet) (4) | −1.30 | −0.58 | 1.10 | |
| $MoO_2$(saet)(py) (5) | −1.30 | −0.58 | 0.98 | |
| $MoO_2$(3-Me-saet) (6) | −1.44 | −0.50 | 0.95 | |
| $MoO_2$(3-*i*-Pr-saet)(Im) (7) | −1.33 | −0.58 | 0.99 | |
| $MoO_2$(3-*t*-Bu-saet)(HMPA) (8) | −1.30 | −0.68 | 0.97 | |
| $MoO_2$(3-Ph-saet)($Me_2SO$) (9) | −1.26 | −0.57 | 1.00 | |
| $MoO_2$(3-OMe-sma) (10) | −1.06 | −0.22 | 1.03 | |
| $MoO_2$(3-*i*-Pr-sma)(py) (11) | −1.10 | −0.20 | 1.00 | |
| $MoO_2$(3-*t*-Bu-sma)(py) (12) | −1.04 | −0.32 | 1.02 | |
| $MoO_2$(3-Ph-sma)(py) (13) | −0.99 | −0.20 | 1.00 | −1.97 |
| $MoO_2(hbeH_2)(Me_2SO)$ (14) | −1.44 | −0.14 | 1.00 | |
| $MoO_2$(3-*t*-Bu-$hbeH_2$)[d] (15) | −1.52 | −0.20 | 1.00 | −2.15 |
| $MoO_2$(3,5-di-*t*-Bu-$hbeH_2$) (16) | −1.58 | −0.15 | 1.00 | |
| $MoO_2$(3,5-di-*t*-Bu-$hbcH_2$) (17) | −1.57 | −0.03 | 1.03 | |
| $MoO_2$(3,5-di-*t*-Bu-$hbmeH_2$) (18) | −1.64 | −0.18 | 1.00 | |
| $MoO_2$(3,5-di-*t*-Bu-$hbpH_2$) (19) | −1.44 | +0.11 | 1.96 | |
| $MoO_2$(3-Ph-$hbeH_2$) (20) | −1.42 | +0.19 | 0.90 | −2.00 |
| $MoO_2(mbeH_2)$ (21) | −1.54 | −0.88 | (2) | |
| $MoO_2(mpeH_2)$[g] | −1.44 | −0.89 | (2) | |
| MoO(3-*t*-Bu-$hbeH_2$)($CH_3OH$) (22) | −1.78 | −0.04 | 0.75[f] | |
| $MoO(mbeH_2)$ (23) | −1.43 | −0.30 | 0.91[f] | |
| $MoO(mpeH_2)$[h] | −1.42 | −0.30 | 0.71[f] | |

[a] Cyclic voltammogram reduction peak. [b] Oxidation peak. [c] $n$ = electrons/molecule, coulometric reduction. [d] MeCN; 0.10 M $[n\text{-}Bu_4N][BF_4]$. [e] Second reduction peak. [f] Coulometric oxidation. [g] Reference 14. [h] Reference 17. All data obtained in DMF, 0.10 M $[Et_4N]Cl$, or $[n\text{-}Bu_4N][BF_4]$, except in d. Scan rate 0.100 V $s^{-1}$.

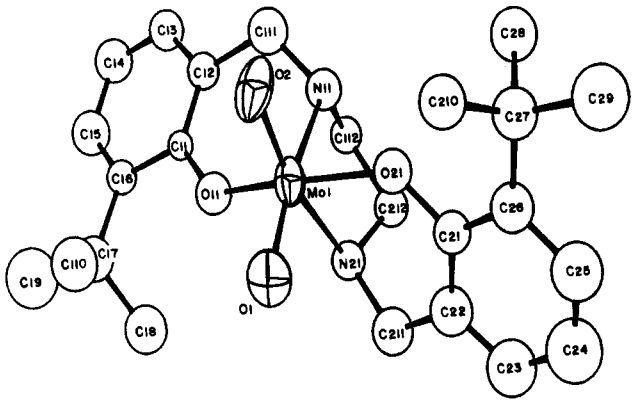


Figure 4. View of $MoO_2$(3-*t*-Bu-$hbeH_2$); hydrogen atoms omitted for clarity.

ecule adopts distorted octahedral geometry, with the N atoms trans to the terminal oxo groups. The average distances, Mo–$O_t$ = 1.708 (6) Å, Mo–$O_l$ = 1.938 (17) Å, and Mo–N = 2.359 (6) Å, are similar to those found in other six-coordinate dioxo–molybdenum(VI) complexes.[16,17]

Figure 4 and molecular models indicate that each terminal oxo group is in close proximity to a *tert*-butyl group of the ligand. In the solid state the distance between a terminal oxo group and the nearest carbon of the adjacent *tert*-butyl group is ~3.9 Å (e.g., O1···C110 and O2···C210). This distance is to be compared to the estimated van der Waals contact for an O···$CH_3$ interaction of 3.6 Å.[18] This partial shielding of the oxo group by the *tert*-butyl group may be an important

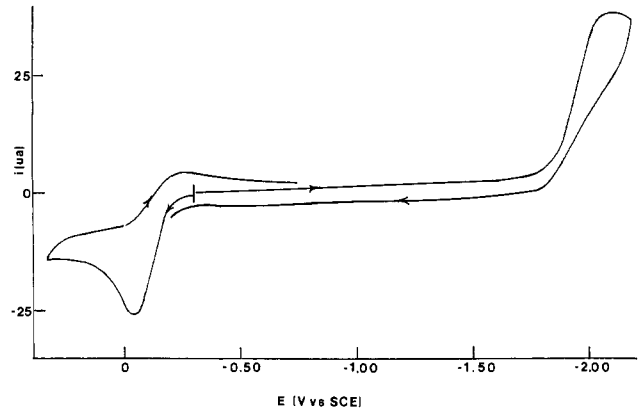


Figure 5. Cyclic voltammogram of MoO(3-*t*-Bu-$hbeH_2$)($CH_3OH$) ($1.04 \times 10^{-3}$ M) (0.100 M $[(n\text{-}Bu)_4N][BF_4]$ in DMF; scan rate 0.100 V $s^{-1}$).

factor in the chemical and electrochemical behavior of $MoO_2LH_2$.

**Mo(IV)–Oxo Complexes (22 and 23).** As seen in Figure 1, a second reduction at a potential <−2.00 V, most likely to an Mo(IV) complex, is present in the CV of $MoO_2$(3-*t*-Bu-$hbeH_2$) (**15**). Because of high background currents, reliable coulometric data for this reduction could not be obtained. Reduction of the complex with excess $[n\text{-}Bu_4N][BH_4]$ in MeOH, however, gave the Mo(IV) complex, MoO(3-*t*-Bu-$hbeH_2$)($CH_3OH$) (**22**). The CV of this complex exhibits both irreversible reduction and oxidation peaks (Figure 5). Coulometric oxidation at 0.10 V removes 0.75 electron/molecule, the EPR spectrum of the oxidized solution indicates 70 ± 10% of a Mo(V) complex present, and the CV of the oxidized solution shows complete oxidation of MoO(3-*t*-Bu-$hbeH_2$)($CH_3OH$). Complex **23**, prepared by reduction of **21** with *p*-thiocresol, shows an oxidation peak at −0.30 V coupled to a reduction peak at −0.45 V in its CV upon scanning in the anodic direction. A cathodic scan shows an additional reduction peak at −1.45 V. The CV is essentially identical with that reported for $MoO(mpeH_2)$.[19] One-electron oxidation at −0.20 V removes 0.91 electron/molecule, giving a solution with 90 ± 10% Mo(V), as determined by EPR. The CV and the EPR and electronic spectra of the oxidized solution are very similar to those reported for $MoOCl(mpeH_2)$[14,20] (Tables III and IV). The EPR spectra, however, are not the same as those obtained by one-electron reduction of **15** and **21**, respectively, and the room-temperature spectra exhibit no $^{14}N$ coupling (Table III). The electronic spectra of the Mo(V) products of **22** and **23** are also quite different from the electronic spectra of the Mo(V) products of **15** and **21** (Table IV).

Upon treatment with 2 equiv of $[n\text{-}Bu_4N]OH$, the EPR (and electronic) spectra of the Mo(V) products of **22** and **23** become identical with the corresponding spectra of the Mo(V) products of **15** and **21**, including the appearance of the five-line splitting of two equivalent $^{14}N$ nuclei at room temperature.

## Discussion

The electrochemical and EPR results indicate considerable steric bulk, as provided by the *tert*-butyl groups in the 3-position of the aromatic rings of complexes **15–18**, is necessary at the cis positions of Mo(VI)–dioxo complexes to prevent dimerization upon one-electron reduction. Additional bulky groups in the 5-position of the aromatic rings, or as substituents of the methylene bridge of the ligand (**16–18**), which might

(16) Berg, J. M.; Hodgson, K. O.; Cramer, S. P.; Corbin, J. L.; Elsberry, A.; Pariyadath, N.; Stiefel, E. I. *J. Am. Chem. Soc.* **1979**, *101*, 2774. Berg, J. M.; Holm, R. H. *Inorg. Chem.* **1983**, *22*, 1768.
(17) Bruce, A.; Corbin, J. L.; Dahlstrom, P. L.; Hyde, J. R.; Minelli, M.; Stiefel, E. I.; Spence, J. T.; Zubieta, J. *Inorg. Chem.* **1982**, *21*, 917.
(18) Pauling, L. "The Nature of the Chemical Bond", 3rd ed.; Cornell University Press: Ithaca, New York, 1960; p 260.
(19) Boyd, I. W.; Spence, J. T. *Inorg. Chem.* **1982**, *21*, 1602.
(20) Spence, J. T.; Minelli, M.; Kroneck, P.; Scullane, M. I.; Chasteen, N. D. *J. Am. Chem. Soc.* **1978**, *100*, 8002. Scullane, M. I.; Taylor, R. D.; Minelli, M.; Spence, J. T.; Yamanouchi, K.; Enemark, J. H.; Chasteen, N. D. *Inorg. Chem.* **1979**, *18*, 3213.

Table III. EPR Parameters[a]

| complex | $g_1$ | $g_2$ | $g_3$ | $g_0$[c] | $^{95,97}$Mo, mT $A_1$ | $A_2$ | $A_3$ | $^{14}$N, mT $A_0$[c] | $A$[c] |
|---|---|---|---|---|---|---|---|---|---|
| [MoO(3-*t*-Bu-hbe)]$^-$[b] ($15^-$) | 1.977 | 1.964 | 1.947 | 1.961 | 3.0 | 7.4 | 3.8 | 4.8 | 0.26 |
| [MoO(3,5-di-*t*-Bu-hbe)]$^-$[b] ($16^-$) | 1.976 | 1.962 | 1.947 | 1.961 | 3.0 | 7.4 | 3.8 | 4.8 | 0.26 |
| [MoO(3,5-di-*t*-Bu-hbc)]$^-$[b] ($17^-$) | 1.977 | 1.962 | 1.947 | 1.962 | 3.0 | 7.4 | 3.7 | 4.7 | 0.21 |
| [MoO(3,5-di-*t*-Bu-hbme)]$^-$[b] ($18^-$) | 1.975 | 1.961 | 1.947 | 1.961 | 3.0 | 7.4 | 3.7 | 4.7 | 0.21 |
| [MoO(mbe)]$^-$[b] ($21^-$) | 2.010 | 1.970 | 1.970 | 1.987 | 6.2 | 2.4 | 2.4 | 3.8 | 0.24 |
| [MoO(mpe)]$^-$[b] | 2.006 | 1.984 | 1.986 | 1.990 | 6.2 | 2.5 | 2.5 | 3.8 | 0.23 |
| [MoO(3-*t*-Bu-hbeH$_2$)]$^+$[d] ($22^+$) | 1.959 | 1.946 | 1.936 | 1.946 | 3.7 | 8.0 | 3.2 | 5.0 | |
| [MoO(mbeH$_2$)]$^+$[d] ($23^+$) | 2.013 | 1.950 | 1.946 | 1.970 | 6.1 | 3.8 | 2.1 | 4.0 | |
| MoOCl(mpeH$_2$)[e] | 2.011 | 1.958 | 1.943 | 1.969 | 6.1 | 4.0 | 2.5 | 4.0 | |

[a] $g$ values and $A_0$, $A_1$, and $A_2$ values obtained from spectra by inspection. $A_3$ calculated from $g_0A_0 = {}^1/_3(g_1A_1 + g_2A_2 + g_3A_3)$. [b] Obtained by electrochemical reduction of corresponding Mo(VI)-dioxo complexes. [c] $g_0$, $A_0$, $^{14}$N, room temperature; all other values, 77 K. [d] Obtained by electrochemical oxidation of corresponding Mo(IV)-oxo complexes. [e] Reference 14. All spectra in DMF, 0.10 M [Et$_4$N]Cl, or [*n*-Bu$_4$N][BF$_4$].

Table IV. Electronic Spectra[a]

| complex | $\lambda_{max}$, nm | log $\epsilon$ |
|---|---|---|
| $MoO_2LH_2$ | | |
| $MoO_2$(3-*t*-Bu-hbeH$_2$) (**15**) | 335 | 3.81 |
| $MoO_2$(3,5-di-*t*-Bu-hbeH$_2$) (**16**) | 345 | 3.86 |
| $MoO_2$(3,5-di-*t*-Bu-hbcH$_2$) (**17**) | 344 | 3.87 |
| $MoO_2$(3,5-di-*t*-Bu-hbmeH$_2$) (**18**) | 345 | 3.78 |
| $MoO_2$(mbeH$_2$) (**21**) | 368 | 3.81 |
| $MoO_2$(mpeH$_2$)[b] | 368 | 3.86 |
| [MoOL]$^-$[c] | | |
| [MoO(3-*t*-Bu-hbe)]$^-$ ($15^-$) | 465 | 2.65 |
| [MoO(3,5-di-*t*-Bu-hbe)]$^-$ ($16^-$) | 438 | sh |
| [MoO(3,5-di-*t*-Bu-hbc)]$^-$ ($17^-$) | 436 | sh |
| [MoO(3,5-di-*t*-Bu-hbme)]$^-$ ($18^-$) | 433 | sh |
| [MoO(mbe)]$^-$ ($21^-$) | 350 | 3.27 |
| [MoO(mpe)]$^-$ | 352 | 3.24 |
| $MoOLH_2$ | | |
| MoO(3-*t*-Bu-hbeH$_2$)(CH$_3$OH) (**22**) | 473 | 3.89 |
| MoO(mbeH$_2$) (**23**) | 364 | 3.32 |
| MoO(mpeH$_2$)[d] | 367 | 3.52 |
| [MoOLH$_2$]$^+$[e] | | |
| [MoO(3-*t*-Bu-hbeH$_2$)]$^+$ ($22^+$) | 332 | 3.76 |
| [MoO(mbeH$_2$)]$^+$ ($23^+$) | 510 | 3.41 |
| MoOCl(mpeH$_2$)[b] | 510 | 3.32 |

[a] DMF, 0.10 M [Et$_4$N]Cl, or [*n*-Bu$_4$N][BF$_4$]. [b] Reference 14. [c] Obtained by one-electron reduction of $MoO_2LH_2$ complexes. [d] Reference 17. [e] Obtained by one-electron oxidation of $MoOLH_2$ complexes.

Table V. Summary of Crystal and Refinement Data for $MoC_{24}H_{34}N_2O_4 \cdot CH_2Cl_2$

| | |
|---|---|
| space group | *Pbca* |
| *a*, Å | 13.728 (4) |
| *b*, Å | 28.48 (1) |
| *c*, Å | 27.50 (2) |
| *V*, Å$^3$ | 10753 (8) |
| *Z* | 16 |
| mol wt (without solvent) | 510.50 |
| $D_{calcd}$, g/cm$^3$ | 1.33 |
| radiation, Å | Mo K$\alpha$ ($\lambda$ = 0.710 73) |
| $\mu$, cm$^{-1}$ | 5.02 |
| cryst dimen, mm | 0.4845 × 0.2574 × 0.0761 |
| cryst faces | (100), (010), (001) |
| transmissn coeff | 0.882–0.962 |
| scan speed, deg/min | variable, 5–15 |
| scan range | 1.0° below K$\alpha_1$ to 1.0° above K$\alpha_2$ |
| peak:bkgd counting time | 2.0:1.0 |
| 2$\theta$ limits, deg | 2.9–45.0 |
| no. of unique reflcns | 9525 |
| no. of unique data used | 2286 with $F_o > 3\sigma(F_o)$ |
| $R_1$ | 0.072 |
| $R_2$ | 0.071 |
| GOF = $\{\Sigma w(\lvert F_o\rvert - \lvert F_c\rvert)^2/(NO - NV)\}^{1/2}$ [a] | 1.8 |

[a] NO = unique data used; NV = number of variables.

exert a buttressing effect, appear to be unnecessary, since the one-electron-reduction product of **15** is as stable toward dimerization as are one-electron-reduced **16–18**. The phenyl group, as a 3-substituent, is not effective in preventing dimerization (**20**), while expansion of the dimethylene bridge to a trimethylene bridge (**19**) gives an EPR-silent species upon reduction. The latter may be a result of lack of coordination of the N atoms in the Mo(V) complex, producing a Mo(V) dioxo-bridged structure with 14-membered rings and monoprotonated nitrogen ligands, $Mo_2O_4(LH)_2$, as has been found for $Mo_2O_4[(SCH_2CH_2N(CH_3)(CH_2)_3N(CH_3)CH_2CH_2S)H]_2$.[17] This was attributed to the lack of steric restraint of the 6-membered ring (trimethylene bridge) as opposed to the analogous 5-membered ring (dimethylene bridge) in enforcing the geometry necessary for bidentate $N_2$ coordination. An examination of a stereo model of the dioxo-bridged structure without N coordination indicates considerably more flexibility in geometry with consequent reduction in steric interaction of ligands. Alternatively, since complete reduction of **19** consumes ~2 electrons/molecule, the lack of an appreciable concentration of Mo(V) after one-electron reduction may be a result of overlap of Mo(VI) and Mo(V) reduction peaks, such that reduction proceeds directly to the Mo(IV) state. This would occur if the Mo(VI/V) potential were more negative than the Mo(V/IV) potential, as has been observed with other Mo complexes.[14,21]

The finding of ~50% Mo(V) present upon one-electron coulometric reduction of **21** and $MoO_2$(mpeh$_2$) may indicate the presence of a monomer–dimer equilibrium, suggesting the ligands are not as effective in preventing dimerization as the ligands of **15–18**. Alternatively, the results may represent competition between one- and two-electron reduction, since complete reduction at this potential consumes 2 electrons/molecule, and the CV after one-electron reduction indicates the presence of ~25% unreduced Mo(VI) complex and exhibits a new peak at 0.08 V more negative, probably for reduction of Mo(V) to Mo(IV). This suggests the difference in reduction potentials for the two processes Mo(VI/V) and Mo(V/IV) is insufficient to effect clean reduction to Mo(V),[21] but sufficient to give a mixture of Mo(VI), Mo(V), and Mo(IV) upon addition of 1 electron/Mo(VI).

The $^{14}$N coupling of 0.26 mT observed in the room-temperature EPR spectra for complexes **15** and **16** indicates two

(21) If the separation of the two reduction peaks, Mo(VI/V) and Mo(V/IV), is quite small, one-electron coulometric reduction may produce a mixture of Mo(VI), -(V), and -(IV) species, depending upon the relative rates of the irreversible processes, while two-electron reduction should result in complete reduction to Mo(IV). Because the processes are irreversible, however, no estimate of the relative amounts of Mo(VI), -(V), and -(IV) at a given degree of reduction is possible in the absence of rate data.

Table VI. Bond Distances (Å) and Bond Angles (deg) for $MoO_2$(3-*t*-Bu-hbe$H_2$)

Molecule 1

| atom 1 | atom 2 | dist | atom 1 | atom 2 | dist |
|---|---|---|---|---|---|
| Mo1 | O1 | 1.706 (10) | Mo1 | O21 | 1.909 (10) |
| Mo1 | O2 | 1.718 (9) | Mo1 | N11 | 2.368 (12) |
| Mo1 | O11 | 1.948 (10) | Mo1 | N21 | 2.356 (12) |

| atom 1 | atom 2 | atom 3 | angle |
|---|---|---|---|
| O1 | Mo1 | O2 | 109.2 (6) |
| O1 | Mo1 | O11 | 94.4 (5) |
| O1 | Mo1 | O21 | 98.5 (5) |
| O1 | Mo1 | N11 | 161.7 (5) |
| O1 | Mo1 | N21 | 90.5 (5) |
| O2 | Mo1 | O11 | 98.8 (4) |
| O2 | Mo1 | O21 | 97.2 (5) |
| O2 | Mo1 | N11 | 88.5 (5) |
| O2 | Mo1 | N21 | 160.2 (5) |
| O11 | Mo1 | O21 | 154.9 (4) |
| O11 | Mo1 | N11 | 77.9 (4) |
| O11 | Mo1 | N21 | 79.9 (4) |
| O21 | Mo1 | N11 | 83.2 (4) |
| O21 | Mo1 | N21 | 78.5 (4) |
| N11 | Mo1 | N21 | 71.9 (4) |

Molecule 2

| atom 1 | atom 2 | dist | atom 1 | atom 2 | dist |
|---|---|---|---|---|---|
| Mo2 | O3 | 1.703 (9) | Mo2 | O41 | 1.951 (12) |
| Mo2 | O4 | 1.707 (10) | Mo2 | N31 | 2.351 (12) |
| Mo2 | O31 | 1.946 (10) | Mo2 | N41 | 2.362 (11) |

| atom 1 | atom 2 | atom 3 | angle |
|---|---|---|---|
| O3 | Mo2 | O4 | 109.2 (5) |
| O3 | Mo2 | O31 | 96.7 (5) |
| O3 | Mo2 | O41 | 99.9 (5) |
| O3 | Mo2 | N31 | 162.5 (5) |
| O3 | Mo2 | N41 | 88.7 (4) |
| O4 | Mo2 | O31 | 98.5 (4) |
| O4 | Mo2 | O41 | 95.4 (5) |
| O4 | Mo2 | N31 | 88.2 (5) |
| O4 | Mo2 | N41 | 161.8 (5) |
| O31 | Mo2 | O41 | 153.5 (4) |
| O31 | Mo2 | N31 | 77.9 (4) |
| O31 | Mo2 | N41 | 82.3 (4) |
| O41 | Mo2 | N31 | 80.1 (4) |
| O41 | Mo2 | N41 | 77.5 (4) |
| N31 | Mo2 | N41 | 74.1 (4) |

equivalent N ligands interacting with the unpaired electron in the $d_{xy}$ orbital of the Mo(V) complex. Similar results have been observed for Mo(V)–oxo complexes with both $N_2S_2$ and $N_2O_2$[10,11] tetradentate ligands, as well as with non-oxo–Mo(V) complexes, having aromatic deprotonated amino (amido) ligands.[22] In this case, however, the amino groups of **15–18**, **21**, and $MoO_2$(mpe$H_2$) are aliphatic with much lower acidity, making deprotonation considerably more difficult. In these cases of $^{14}N$ coupling to Mo(V) EPR signals, the amino ligands are deprotonated (trigonal, $sp^2$ N), with coupling constants of ~0.25 mT.[10,22] In the case of $[Mo(R_2dtc)_2(NO)_2]^-$, in which the N bonding may be approximately described as sp, $^{14}N$ splittings of 0.72–1.02 mT were observed,[23] while Bray has reported $^{14}N$ coupling of 0.36 mT in an alloxanthine–xanthine oxidase complex,[24] arising from a trigonal (but neutral) nitrogen of the alloxanthine. These results suggest the magnitude of the $^{14}N$ coupling depends on N-bond hybridization in complexes with comparable geometries, with sp > $sp^2$ > $sp^3$. Since no $^{14}N$ couplings from $sp^3$ N ligands to Mo(V) EPR signals have been reported, such couplings may be <0.10 mT and not easily observable. If this is the case, the Mo(V) complexes obtained by one-electron reduction of the Mo(VI)–dioxo complexes reported here have deprotonated nitrogens, are formulated as anions (e.g., $[MoO(3\text{-}t\text{-Bu-hbe})]^-$) (Table III), and as such are analogous to Mo(V)–oxo complexes with deprotonated aromatic amino ligands reported earlier.[10] This formulation is supported by the results with the $Mo^{IV}OLH_2$ complexes **22** and **23**. One-electron oxidation of these complexes in aprotic solvents gives 70–90% Mo(V) monomers, which have smaller EPR *g* values, slightly higher *A* values, and no $^{14}N$ superhyperfine splitting, as well as different electronic spectra. It is clear **23** and its one-electron-oxidation product are completely analogous to the known MoO(mpe$H_2$)[19] and MoOCl(mpe$H_2$)[14] complexes, respectively, both of which have normal (protonated) amino groups (the Mo(V) EPR spectrum of MoOCl(mpe$H_2$) also does not exhibit $^{14}N$ coupling[20]). The interconversion of the one-electron-reduced products of **15** and **21** with the one-electron-oxidized products of **22** and **23**, respectively, upon addition of $H^+$ or $OH^-$ argues strongly for the formulation of the Mo(V) complexes at **15** and **21** as having deprotonated ligands:

$$MoO_2LH_2 \xrightarrow{e^-} MoOL^- + H_2O$$

$$2OH^- \rightleftharpoons 2H^+$$

$$MoOLH_2 \xrightarrow{-e^-} MoOLH_2^+$$

Finally, one-electron coulometric reduction of the analogous known complex $MoO_2(SCH_2CH_2N(CH_3)CH_2CH_2N(CH_3)CH_2CH_2S)_2$, which cannot undergo deprotonation, gives a weak (~10%) Mo(V) EPR signal with no $^{14}N$ coupling, as determined in this laboratory and also reported by Pickett et al.[25]

It therefore appears that one-electron electrochemical reduction of $MoO_2LH_2$ complexes with tetradentate $N_2O_2$ or $N_2S_2$ ligands that, because of steric factors, cannot undergo dimerization, proceeds with deprotonation of the amino groups of the ligands and elimination of $H_2O$, even when the amino groups are aliphatic. On the other hand, synthesis from Mo(V)–oxo starting materials, or one-electron electrochemical oxidation of Mo(IV)–oxo complexes with the same aliphatic amino ligands, in which the removal of oxo is not required, gives normal (i.e., protonated) complexes:

$$MoO_2LH_2 \xrightarrow{e^-} MoOL^- + H_2O$$

$$MoOCl_3 + LH_4 \rightarrow MoOClLH_2 + 2HCl$$

$$MoOLH_2 \xrightarrow{-e^-} MoOLH_2^+$$

This is a remarkable demonstration of the ability of Mo(V) to greatly increase the acidity of coordinated ligands and appears to be a general phenomenon. With aromatic amino ligands, as a result of their greater acidity, only deprotonated Mo(V)–oxo complexes are obtainable, either by reduction of Mo(VI)–dioxo complexes or by synthesis.[10] Two-electron reduction, at least for **21**, which gives the deprotonated Mo(V)–oxo intermediate, appears to result in decomposition, possibly because the lower charge on Mo makes the deprotonated form unstable.

The presence of two equivalent $^{14}N$ ligands indicates the Mo(V) complexes **15**, **16**, **21**, and $[MoO(mpe)]^-$ are most likely square pyramidal in structure with the trans position occupied by $Cl^-$ or solvent:

(22) (a) Gardner, J. K.; Pariyadath, N.; Corbin, J. L.; Stiefel, E. I. *Inorg. Chem.* **1978**, *17*, 897. (b) Pariyadath, N.; Newton, W. E.; Stiefel, E. I. *J. Am. Chem. Soc.* **1976**, *98*, 5388.

(23) Budge, J. A.; Broomhead, J. A.; Boyd, P. D. W. *Inorg. Chem.* **1982**, *21*, 1031.

(24) Williams, J. W.; Bray, R. C. *Biochem. J.* **1981**, *195*, 753.

(25) Pickett, C.; Kumar, S.; Vella, P. A.; Zubieta, J. *Inorg. Chem.* **1982**, *21*, 908.

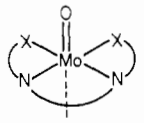

X = O, S

Complexes **17** and **18** have unsymmetrical dimethylene bridges, resulting in nonequivalent N ligands, as observed in their room-temperature EPR spectra; their structures are likely to be the same as **15** and **16**, however, since coordination of a N trans to oxo, with little overlap of N orbitals with the Mo $d_{xy}$ orbital, would result in coupling of only one $^{14}N$ (three lines). Analysis of EPR results for the protonated complex $MoOCl(mpeH_2)$ favors a cis (chloro) structure,[20] which is also likely true for $[MoO(mbeH_2)]^+$ in the presence of $[Et_4N]Cl$.

The Mo(V) EPR spectra of most of the Mo enzymes exhibit coupling of one or two $^1H$ nuclei.[2,6] This is generally ascribed to $OH^-$ or $SH^-$ protons, the $OH^-$ or $SH^-$ ligands arising by reduction of oxo or sulfido Mo ligands.[2,5,6] Recent EPR results from xanthine oxidase, however, suggest at least one of the protons coupled to the Mo(V) center may be associated with a protein side chain (possibly an amino group) rather than an $OH^-$ or $SH^-$ ligand.[26] The only known cases of such $^1H$ coupling to Mo(V) EPR signals in model complexes are those with monodeprotonated amino (trigonal) ligands, and these complexes also exhibit $^{14}H$ coupling of ~0.20–0.26 mT.[22] The results reported here suggest an alternate origin for at least one of the observed $^1H$ splittings in the Mo(V) EPR of the enzymes: a deprotonated aliphatic amino ligand on Mo, in which $^{14}N$ coupling is not observable because of the line width of the enzyme spectra.

The results demonstrate Mo(V) oxo-bridged dimer formation upon reduction of Mo(VI)–dioxo complexes may be avoided by proper ligand design, thus mimicking the Mo centers of the enzymes. The synthesis of complexes such as **15** with the corresponding sulfur ligands, and with other NOS ligands having sterically bulky properties, is under way. Such ligands should shift the reduction potentials to more positive values, making the Mo(V) and -(IV) states more accessible for electrochemical investigation and consequently more suitable models for reaction with substrates.

## Experimental Section

**Starting Materials and Reagents.** Reagent grade solvents, distilled and dried by standard methods, were used in all cases.

Isobutyraldehyde, 2-ethylbutyraldehyde, ethylamine, methylamine, ethylenediamine, 1,3-propylenediamine, 2-methyl-1,2-propylenediamine, acetylacetone, paraformaldehyde, imidazole, 2-aminoethanethiol, 2-methoxyphenol, 2-methylphenol, 2-isopropylphenol, 2-*tert*-butylphenol, 2,4-di-*tert*-butylphenol, 2-phenylphenol, salicylaldehyde, 2-aminothiophenol, and tetra-*n*-butylammonium tetrafluoroborate were purchased from Aldrich Chemical Co. 1,2-Diaminocyclohexane (cis–trans mixture) was obtained from Strem Chemicals, Inc., tetra-*n*-butylammonium borohydride from Fluka, tetraethylammonium chloride from Eastman, and $Na_2MoO_4 \cdot 2H_2O$ from J. T. Baker.

The 3- and 3,5-substituted 2-hydroxybenzyaldehydes were prepared by the procedure of Gasiraghi et al.[27]

**Syntheses. Ligands.** The ligands $MeNHCH_2CEt_2SH$, $EtNHCH_2Et_2SH$, $EtNHCH_2CMe_2SH$, and $mbeH_4$ were prepared by published procedures.[28] Yields of 60–70% were obtained.

The 3-substituted $smaH_2$ ligands were prepared as described in the literature.[10]

**3-*t*-Bu-hbeH$_4$.** Ethylenediamine (3.10 g, 0.05 mol) was added dropwise with stirring to a solution of 17.8 g (0.10 mol) of freshly distilled 2-hydroxy-3-*tert*-butylbenzaldehyde in 300 mL of MeOH. After addition was complete, the solution was stirred for 3 h at room temperature, during which time the yellow-orange Schiff base appeared as a solid. The precipitate was collected by filtration, washed with

**Table VII.** Positional Parameters and Their Estimated Standard Deviations for $MoO_2(3\text{-}t\text{-Bu-hbeH}_2)$

| atom | *x* | *y* | *z* | $B$,[a] Å$^2$ |
|---|---|---|---|---|
| Mo1 | 0.0672 (1) | 0.18065 (5) | 0.23344 (4) | 3.28 (3) |
| O1 | 0.1873 (8) | 0.1949 (5) | 0.2277 (5) | 4.7 (4) |
| O2 | 0.058 (1) | 0.1241 (4) | 0.2548 (4) | 5.2 (3) |
| O11 | 0.491 (9) | 0.1682 (4) | 0.1644 (4) | 3.5 (3)* |
| O21 | 0.414 (9) | 0.2117 (4) | 0.2936 (5) | 3.5 (3)* |
| N11 | −0.105 (1) | 0.1824 (5) | 0.2259 (4) | 3.5 (4)* |
| N21 | 0.022 (1) | 0.2561 (5) | 0.2065 (4) | 3.1 (3)* |
| C11 | −0.140 (8) | 0.1453 (5) | 0.1361 (6) | 1.8 (1)* |
| C12 | −0.105 (1) | 0.1313 (6) | 0.1516 (7) | 2.9 (4)* |
| C13 | −0.165 (1) | 0.1073 (7) | 0.1193 (8) | 3.7 (5)* |
| C14 | −0.140 (2) | 0.0998 (7) | 0.0725 (8) | 4.4 (5)* |
| C15 | −0.048 (2) | 0.1144 (7) | 0.0574 (7) | 4.5 (5)* |
| C16 | 0.015 (1) | 0.1367 (6) | 0.0878 (4) | 2.5 (2)* |
| C17 | 0.116 (1) | 0.1508 (7) | 0.0703 (8) | 4.5 (4)* |
| C18 | 0.136 (2) | 0.2042 (8) | 0.0739 (8) | 5.2 (6)* |
| C19 | 0.136 (2) | 0.1365 (9) | 0.0196 (8) | 8.3 (8)* |
| C110 | 0.195 (2) | 0.1283 (8) | 0.1020 (7) | 5.8 (6)* |
| C111 | −0.140 (2) | 0.1394 (7) | 0.2038 (5) | 4.5 (3)* |
| C112 | −0.141 (1) | 0.2246 (6) | 0.2001 (6) | 2.9 (2)* |
| C21 | 0.073 (2) | 0.2532 (6) | 0.3144 (3) | 3.3 (3)* |
| C22 | 0.097 (1) | 0.2916 (7) | 0.2845 (8) | 4.6 (5)* |
| C23 | 0.123 (2) | 0.3326 (8) | 0.3062 (8) | 6.1 (5)* |
| C24 | 0.127 (2) | 0.3350 (9) | 0.3561 (8) | 7.4 (7)* |
| C25 | 0.105 (2) | 0.2966 (8) | 0.3850 (9) | 5.9 (6)* |
| C26 | 0.076 (2) | 0.2541 (7) | 0.3641 (7) | 4.2 (2)* |
| C27 | 0.051 (2) | 0.2123 (7) | 0.3977 (7) | 4.4 (5)* |
| C28 | −0.056 (2) | 0.1996 (7) | 0.3905 (8) | 4.9 (5)* |
| C29 | 0.056 (2) | 0.2242 (8) | 0.4517 (8) | 6.4 (5)* |
| C210 | 0.118 (1) | 0.1696 (7) | 0.3868 (8) | 4.4 (4)* |
| C211 | 0.089 (1) | 0.2911 (7) | 0.2300 (7) | 4.5 (5)* |
| C212 | −0.081 (1) | 0.2663 (6) | 0.2186 (6) | 3.3 (2)* |
| Mo2 | 0.0707 (1) | −0.05405 (5) | 0.26316 (5) | 3.35 (2) |
| O3 | −0.0493 (8) | −0.0510 (4) | 0.2477 (3) | 3.8 (2) |
| O4 | 0.094 (1) | −0.1072 (4) | 0.2894 (4) | 4.6 (4) |
| O31 | 0.0614 (9) | −0.0164 (4) | 0.3221 (4) | 3.4 (2)* |
| O41 | 0.1268 (9) | −0.0702 (4) | 0.2002 (5) | 4.0 (2)* |
| N31 | 0.2344 (9) | −0.0340 (5) | 0.2774 (4) | 3.0 (2)* |
| N41 | 0.0934 (9) | 0.0203 (5) | 0.2269 (94) | 2.7 (3)* |
| C31 | 0.111 (1) | −0.0088 (7) | 0.3637 (7) | 3.5 (4)* |
| C32 | 0.206 (1) | −0.0240 (6) | 0.3672 (6) | 2.7 (2)* |
| C33 | 0.256 (2) | −0.0180 (7) | 0.4133 (8) | 4.9 (5)* |
| C34 | 0.212 (2) | 0.0019 (7) | 0.4498 (8) | 4.5 (5)* |
| C35 | 0.118 (1) | 0.0183 (8) | 0.4452 (8) | 5.0 (5)* |
| C36 | 0.063 (1) | 0.0146 (6) | 0.4034 (6) | 3.0 (3)* |
| C37 | −0.044 (1) | 0.0320 (7) | 0.3968 (6) | 3.9 (5)* |
| C38 | −0.073 (2) | 0.0605 (9) | 0.4430 (7) | 7.2 (5)* |
| C39 | −0.057 (2) | 0.0638 (7) | 0.3523 (5) | 4.4 (4)* |
| C310 | −0.109 (2) | −0.0094 (8) | 0.3914 (9) | 5.5 (6)* |
| C311 | 0.263 (1) | −0.0485 (7) | 0.3277 (6) | 3.9 (3)* |
| C312 | 0.249 (1) | 0.0166 (6) | 0.2673 (7) | 3.7 (4)* |
| C41 | 0.1086 (9) | −0.0447 (7) | 0.1530 (7) | 3.5 (4)* |
| C42 | 0.071 (1) | −0.0126 (7) | 0.1436 (6) | 4.0 (4)* |
| C43 | 0.052 (2) | −0.0016 (7) | 0.0947 (8) | 5.2 (6)* |
| C44 | 0.076 (2) | −0.0327 (8) | 0.0588 (6) | 5.8 (5)* |
| C45 | 0.122 (2) | −0.0740 (9) | 0.0676 (9) | 7.0 (7)* |
| C46 | 0.139 (1) | −0.0885 (6) | 0.1165 (7) | 3.6 (4)* |
| C47 | 0.193 (1) | −0.1334 (7) | 0.1281 (4) | 3.8 (4)* |
| C48 | 0.293 (2) | −0.1216 (9) | 0.1503 (7) | 6.1 (5)* |
| C49 | 0.143 (2) | −0.1652 (9) | 0.1631 (7) | 6.7 (5)* |
| C410 | 0.212 (2) | −0.163 (1) | 0.082 (1) | 10 (1)* |
| C411 | 0.042 (1) | 0.0237 (7) | 0.1807 (7) | 3.7 (4)* |
| C412 | 0.201 (1) | 0.0320 (6) | 0.2222 (5) | 3.3 (2) |
| Cl1 | 0.443 (3) | 0.373 (1) | 0.429 (1) | 15 (1)* |
| Cl1′ | 0.348 (2) | 0.237 (1) | 0.454 (1) | 12.9 (9)* |
| Cl2′ | 0.433 (3) | 0.329 (1) | 0.399 (1) | 18 (1)* |
| Cl2 | 0.398 (2) | 0.290 (1) | 0.425 (1) | 12.6 (9)* |

[a] Starred atoms were refined isotropically. Anisotropically refined atoms are given in the form of the isotropic equivalent thermal parameter defined as $8\pi^2(U_{11} + U_{22} + U_{33})/3$.

(26) Barber, M. J.; Siegel, L. M. *Chem. Uses of Molybdenum, Proc. Int. Conf.* **1982**, *4*, 173.
(27) Gasiraghi, G.; Casnati, G.; Cornia, M.; Pochini, A.; Puglia, G.; Sartori, G.; Ungaro, R. *J. Chem. Soc., Perkin Trans.* **1978**, 318.
(28) Corbin, J. L.; Work, D. E. *J. Org. Chem.* **1976**, *41*, 489. D'Amico, J. J.; Dahl, W. E. *Ibid.* **1975**, *40*, 1224, 6951.

20 mL of *n*-hexane, and dried in vacuo at room temperature; yield 15.3 g (80%). The Schiff base was used without further purification. A solution of 7.6 g (0.02 mol) of the Schiff base in 200 mL of dry THF was added dropwise to a solution of 1.90 g of $LiAlH_4$ in 50 mL of dry, deaerated THF in a 3-neck flask with a condenser under Ar at room temperature over 1 h. After the vigorous reaction had subsided, the solution was refluxed for 2 h under Ar. The flask was cooled below 0 °C in dry ice–acetone and carefully hydrolyzed by the addition of 100 mL of 1:1 THF:$H_2O$. After the mixture was stirred for 1 h at room temperature, 5 mL of cold 1:1 $H_2SO_4$:$H_2O$ was added and the mixture stirred for 0.5 h. It was neutralized with 10% NaOH and extracted with $CHCl_3$. The solvent was removed with a rotary evaporator and the white solid dissolved in $CHCl_3$ and dried over $Na_2SO_4$. Solvent was removed and the white solid dried in vacuo for 3 h at room temperature; yield 4.5 g (59%).

**hbeH$_4$, 3,5-di-*t*-Bu-hbeH$_4$, 3,5-di-*t*-Bu-hbcH$_4$, 3,5-di-*t*-Bu-hbmeH$_4$, 3,5-di-*t*-Bu-hbpH$_4$, and 3-Ph-hbeH$_4$** were prepared by the same procedure as 3-*t*-Bu-hbeH$_4$, starting with the appropriate substituted 2-hydroxybenzaldehyde and diamine; yields 40–60%.

Ligand syntheses were monitored by IR spectroscopy, NMR, and TLC to ensure desired compounds were obtained.

**Complexes.** $MoO_2(acac)_2$ was synthesized by the method of Newton and McDonald,[12] $MoO_2(NH_2CH_2CH_2SH)_2$ by the method of Kay and Mitchell,[29] and $MoO_2(mbeH_2)$, $MoO_2(mpeH_2)$, and $MoO_2(mee)$ as described by Taylor et al.[14]

**$MoO_2(MeNHCH_2CEt_2S)_2$ (1).** MeNHCHC(Et)$_2$SH (0.90 g, 6.0 mmol) was added dropwise to a stirred solution of 0.93 g (2.85 mmol) of $MoO_2(acac)_2$ in 30 mL of $CH_2Cl_2$ under $N_2$. After 0.5 h, the solvent was removed under vacuum and the bright yellow residue washed several times with 10-mL portions of diethyl ether and dried in vacuo at room temperature; yield 0.85 g (70%).

**$MoO_2(EtNHCH_2CEt_2S)_2$ (2) and $MoO_2(EtNHCH_2CMe_2S)_2$ (3)** were obtained by the same method as for **1**; yield 80% and 83%, respectively.

**$MoO_2$(saet) (4).** Salicylaldehyde (1.25 g, 0.01 mol) was added to a slurry of 1.40 g (5 mmol) of $MoO_2(NH_2CH_2CH_2SH)_2$ in 50 mL of MeOH and the mixture stirred at room temperature for 4 h. The red-orange solid that formed was removed by filtration, washed with small portions (10 mL) of MeOH and diethyl ether, and dried in vacuo at room temperature; yield 1.35 g (80%).

**$MoO_2$(3-Me-saet), $MoO_2$(3-*i*-Pr-saet), $MoO_2$(3-*t*-Bu-saet), and $MoO_2$(3-Ph-saet)** were obtained by the same method as for $MoO_2$(saet); yields 78%, 86%, 95%, 97%, respectively.

**$MoO_2$(saet)(py) (5).** $MoO_2$(saet) (0.30 g, 1 mmol) was dissolved in 2.5 mL of pyridine. The pyridine was removed under vacuum at room temperature, and the yellow solid was washed with small portions (10 mL) of diethyl ether and air-dried; yield 0.37 g (97%).

**$MoO_2$(3-Me-saet)(py) (6).** This complex was prepared in the same manner as **5**; yield 94%.

**$MoO_2$(3-*i*-Pr-saet)(Im) (7).** This complex was obtained by the addition of 0.70 g (2.0 mmol) of $MoO_2$(3-*i*-Pr-saet) to a solution of 0.15 g (2.0 mmol) of imidazole in 30 mL of MeOH. After stirring for 1 h at room temperature, the solution was placed in the freezer for 2 h. The yellow crystals that formed were removed by filtration, washed with MeOH (10 mL) and diethyl ether (30 mL), and dried in vacuo at room temperature; yield 0.80 g (95%).

**$MoO_2$(3-*t*-Bu-saet)(HMPA) (8).** HMPA (0.75 g) was added to a suspension of 1.45 g (4.0 mmol) of $MoO_2$(3-*t*-Bu-saet) in 20 mL of $CH_2Cl_2$ and the mixture stirred until a clear yellow solution was obtained. Solvent was removed with the rotary evaporator, the yellow solid triturated with five 10-mL portions of diethyl ether, and dried in vacuo at room temperature; yield 1.80 g (82%).

**$MoO_2$(3-Ph-saet)($Me_2SO$) (9).** $MoO_2$(3-Ph-saet) (0.77 g, 2 mmol) was dissolved in 10 mL of $Me_2SO$. Diethyl ether (5 mL) was added dropwise and the solution allowed to stand overnight. The bright yellow precipitate was removed by filtration, washed with small portions (10 mL) of diethyl ether, and dried in vacuo at room temperature; yield 0.78 g (85%).

**$MoO_2$(3-Ph-sma)(py) (13).** $MoO_2(acac)_2$ (0.65 g, 2.0 mmol) in 10 mL of $CH_2Cl_2$ was mixed with 0.63 mg (2.0 mmol) of the Schiff base (3-Ph-smaH$_2$) in 25 mL of $CH_2Cl_2$ and the mixture stirred at room temperature for 0.5 h. The dark brown precipitate that formed was filtered off, washed with small portions of diethyl ether, and dried in vacuo at room temperature. The crude product was dissolved in 10 mL of pyridine and diethyl ether added dropwise until a slight cloudiness was obtained. The mixture was kept overnight in the freezer, and the bright red-orange crystals were filtered off, washed with small portions of diethyl ether, and dried in vacuo at room temperature; yield 0.85 g (80%).

**$MoO_2$(3-*t*-Bu-sma)(py) (12) and $MoO_2$(3-*i*-Pr-sma)(py) (11)** were prepared in the same manner as **13**; yields 73% and 80%, respectively.

**$MoO_2$(3-OMe-sma) (10).** $MoO_2(acac)_2$ (1.30 g, 4.0 mmol) in 20 mL of $CH_2Cl_2$ was added to 1.05 g (4.0 mmol) of the Schiff base (3-OMe-smaH$_2$) in 50 mL of $CH_2Cl_2$ and the mixture stirred for 1 h at rt. The solvent was removed on the rotary evaporator and the red-orange solid washed with three 15-mL portions of diethyl ether and dried in vacuo at room temperature; yield 1.35 g (87%).

**$MoO_2$(hbeH$_2$)($Me_2SO$) (14).** The ligand hbeH$_4$ (1.30 g, 4.0 mmol) was added to 1.20 g (4.4 mmol) of $MoO_2(acac)_2$ in 50 mL of MeOH, and the mixture was refluxed for 1 h. After cooling, the bright yellow solid was removed by filtration and washed with MeOH (10 mL) and diethyl ether (20 mL). It was dried in vacuo at room temperature overnight; yield 1.40 g (88%). The product (0.70 g) was dissolved in 25 mL of 1:4 $Me_2SO$:MeCN, and the solution was kept in the freezer overnight. The bright yellow solid was removed by filtration and dried in vacuo at room temperature overnight.

**$MoO_2$(3-*t*-Bu-hbeH$_2$) (15).** The ligand 3-*t*-Bu-hbeH$_4$ (1.60 g, 4.2 mmol) was added to 1.30 g (4.0 mmol) of $MoO_2(acac)_2$ in 50 mL of dry MeOH and the mixture refluxed for 1.5 h. The solution was cooled to room temperature and allowed to stand for 2 h. Bright yellow needles separated and were filtered off, washed with small portions of diethyl ether, and dried in vacuo at room temperature overnight; yield 1.15 g (56%).

**$MoO_2$(3,5-di-*t*-Bu-hbeH$_2$) (16).** This complex was prepared in the same manner as **15** except absolute EtOH was used in place of MeOH and reflux was carried out for 1 h; yield 85%.

**$MoO_2$(3,5-di-*t*-Bu-hbcH$_2$) (17).** This complex was prepared in the same manner as **15**, except it was refluxed for 0.75 h, the volume was reduced by 50% after cooling, and the solution was allowed to stand overnight in the freezer before filtration; yield 10%.

**$MoO_2$(3,5-di-*t*-Bu-hbmeH$_2$) (18).** This complex was prepared in the same manner as **15** except reflux was carried out for 0.5 h; yield 50%.

**$MoO_2$(3,5-di-*t*-Bu-hbpH$_2$) (19).** This complex was prepared in the same manner as **16**; yield 57%.

**$MoO_2$(3-Ph-hbeH$_2$) (20).** This complex was prepared in the same manner as **15**, except reflux was carried out for 2 h; yield 90%.

**$MoO_2$(mbeH$_2$) (21).** $MoO_2(acac)_2$ (0.98 g, 3.0 mmol) was dissolved in 30 mL of $CH_2Cl_2$, and 0.90 g (3.1 mmol) of the ligand mbeH$_4$ was added and the solution stirred at room temperature for 15 min, during which time bright yellow crystals formed. They were collected by filtration, washed with five 10-mL portions of diethyl ether, and dried in vacuo overnight; yield 90%.

**MoO(3-*t*-Bu-hbeH$_2$)($CH_3OH$) (22).** [(*n*-Bu)$_4$N][BH$_4$] (1.56 g, 6.0 mmol) was added under $N_2$ to 1.0 g (2.0 mmol) of $MoO_2$(3-*t*-Bu-hbeH$_2$) in 50 mL of dry, deaerated MeOH and the solution stirred under $N_2$ for 4 h. The initial yellow solution changed to deep red-brown. After the mixture was allowed to stand overnight at room temperature under $N_2$, a deep red-brown solid precipitated. The product was collected by filtration washed with cold, deaerated diethyl ether (10 mL) under $N_2$, and dried in vacuo at room temperature overnight.

**MoO(mbeH$_2$) (23).** [Et$_4$N][MoO(SC$_6$H$_4$CH$_3$)$_5$] (1.50 g, 2.4 mmol) was dissolved in 30 mL of deaerated, dry MeCN, and 0.73 g (2.5 mmol) of the ligand mbeH$_4$ in 10 mL MeCN was added and the solution refluxed for 25 min with stirring under $N_2$. A crystalline orange-red compound separated out and was collected by filtration, washed with two 10-mL portions of MeCN and dried in vacuo overnight; yield 95%.

**Electrochemistry.** Cyclic voltammetry and coulometry were performed in DMF, MeCN (Burdick and Jackson, dried over molecular sieves), or $CH_2Cl_2$ (distilled, dried) with [Et$_4$N]Cl or [*n*-Bu$_4$][BF$_4$] as electrolytes, using a 3-electrode cell described previously[14] and a PAR Model 173 potentiostat, Model 174 polarographic analyzer, and Model 175 signal generator. Potential measurements have a precision of ±0.005 V, and *n* (coulometric measurements) has a precision of ±0.10.

**EPR.** EPR spectra were obtained with a Varian E-109 spectrometer. Samples were obtained under $N_2$, transferred to EPR tubes

(29) Kay, A.; Mitchell, P. C. H. *J. Chem. Soc. A* **1970**, 2421.

with gas-tight syringes under $N_2$, and frozen immediately in liquid $N_2$. Room-temperature spectra were obtained with a flat cell under Ar. Estimates of spin concentrations were made by using known Mo(V) complexes ($K_3[Mo(CN)_8]$, $MoOCl(thiooxine)_2$)[14] as standards. Estimates of $g$ and $A$ values were made by inspection of the measured spectra, using DPPH as standard.

**Crystal Preparation.** Crystals of the title compound $MoO_2(hbeH_2)$ were grown from dichloromethane. The compound crystallized as very thin rectangular plates. A plate was selected with dimensions in Table V and was mounted on the tip of a slim glass fiber with epoxy.

**Crystallographic Data.** The determination of the Bravais lattice and cell dimensions and the collection of intensity data were carried out with a Syntex $P2_1$ diffractometer equipped with a graphite monochromator. The cell constants were determined on the basis of the centering of 24 reflections with $9° < 2\theta(Mo\ K\alpha) < 19°$. After least-squares refinement of the setting angles, the crystal system and axis lengths were checked by using axial photographs. Several $\omega$ scans showed sharp Bragg peaks, width at half-height 0.27. The crystal and diffractometer data are listed in Table V. Data collection was carried out at room temperature with Mo K$\alpha$ radiation using a $\theta$–$2\theta$ scan technique. An octant of data was collected, $hkl$, out to $2\theta = 45°$. The intensities of two standard reflections, measured every 98 reflections. showed no significant decay during data collection. The data revealed systematic absences unique to the nonstandard space group *Pcab*, which was transformed to the standard space group *Pbca* prior to structure solution. The data were corrected for Lorentz and polarization effects and were also corrected for absorption by the Gaussian integration method.

**Solution and Refinement.** The structure determination and refinement were carried out with the SDP series of crystallographic programs on a PDP 11/34a computer.[30] MULTAN yielded the position of the two independent molybdenum atoms. Subsequent difference Fourier techniques were used to locate the remaining independent non-hydrogen atoms of each molecule. Isotropic refinement of both molecules yielded $R_1 = 0.11$ and $R_2 = 0.13$. A difference map revealed the presence of a disordered dichloromethane molecule. The disorder model that was decided upon structurally resembles a staggered 1,2-dichloroethane molecule. However, the carbon–carbon bond is replaced by one carbon–chlorine bond from each of the disordered dichloromethane molecules. The solvent molecule was assigned an occupancy of 0.5 on the basis of a refinement of the occupancy factor of the chlorine atoms, which were not disordered with the carbon atoms. Refinement was continued with this disorder model and anisotropic thermal parameters for the molybdenum atoms and the oxo oxygen atoms. All the hydrogen atom positions were assigned an arbitrary isotropic thermal value of $B = 5.0$ Å.[2,31] These conditions gave final residual indices of $R_1 = 0.072$ and $R_2 = 0.071$ where refinement was based on the minimization of $\sum w(|F_o| - |F_c|)^2$ where $w^{-1} = \sigma(F_o) + 0.25(cF_o)^2$ with $c = 0.03$. The highest peak from the final difference map was 1.1 e Å$^{-3}$. The final fractional coordinates and thermal parameters of the refined atoms are listed in Table VII. The idealized hydrogen atom positions and a listing of the observed and calculated structure factors are available in the supplementary material.

**Acknowledgment.** The structure was determined in the Molecular Structure Laboratory of the University of Arizona, and we thank S. Merbs for assistance with portions of the structural studies. Financial support of this work by NIH Grant GM 08347 (J.T.S.) and ES 00966 (J.H.E.) is gratefully acknowledged.

**Supplementary Material Available:** Listings of calculated hydrogen atom positions, general temperature factor expressions, thermal parameters, and structure factors for $MoO_2(3\text{-}t\text{-}Bu\text{-}hbeH_2)$ (17 pages). Ordering information is given on any current masthead page.

(30) Computer program used for this analysis were: The Structure Determination Package (SDP) (B. A. Frenz & Associates, Inc., College Station, TX and Enraf-Nonius, Delft, Holland); MULTAN 80 (P. Main et al., University of York, York, England); ORTEP 2 (Johnson, C. K. Report ORNL-3794 Oak Ridge National Laboratory, Oak Ridge, TN). Both MULTAN 80 and ORTEP 2 are included in the SDP software.

(31) Churchill, M. R. *Inorg. Chem.* **1973**, *12*, 1213.

Contribution No. 6898 from the Arthur Amos Noyes Laboratory, California Institute of Technology, Pasadena, California 91125

# Binuclear Complexes of Palladium(II) Containing 1,8-Diisocyano-*p*-menthane

CHI-MING CHE, FRANK H. HERBSTEIN, WILLIAM P. SCHAEFER, RICHARD E. MARSH, and HARRY B. GRAY*

*Received August 24, 1983*

Well-characterized binuclear isocyano complexes of palladium(II) are obtained with the bridging ligand 1,8-diisocyano-*p*-menthane (DMB). The ion $[Pd_2(DMB)_4]^{4+}$ reacts with X ($Cl^-$ or $Br^-$) to give $[Pd_2(DMB)_4X]^{3+}$, where the X is positioned between the metal atoms, encapsulated in the complex. Reaction with $I^-$ leads to an entirely different product, $Pd_2(DMB)_2I_4$, which has been characterized by X-ray crystallography: $Pd_2C_{24}N_4H_{36}I_4$ crystallizes in the monoclinic space group $P2_1/n$ with $a = 11.766$ (4) Å, $b = 15.123$ (8) Å, $c = 9.703$ (2) Å, $\beta = 93.93$ (2)°, and $Z = 2$. The Pd atoms are square-planar coordinated to two CN groups and two I atoms; the DMB ligands are disordered across a center of symmetry. The coordination planes of the Pd atoms are tilted 35° from the perpendicular to the Pd–Pd vector, and a fifth (axial) site is occupied by an I atom from the other half of the dimer. The Pd···Pd distance, 4.582 (1) Å, is such that the ion $[Pd_2(DMB)_4]^{4+}$ can accommodate a $Br^-$ or $Cl^-$ ion between the Pd atoms.

## Introduction

We have been studying for many years the spectroscopic and structural properties of $d^8$-metal–isocyanide complexes.[1-3] Rhodium(I) and iridium(I) complexes have been extensively investigated, but studies involving nickel(II), palladium(II), and platinum(II) have lagged because these divalent metals catalyze polymerization, hydrolysis, and dealkylation reactions of isocyanides.[4-6] One method of avoiding these side reactions during synthesis is to use diisocyanide ligands that can bridge between two metal atoms to form binuclear species; one

(1) Mann, K. R.; Thich, J. A.; Bell, R. A.; Coyle, C. L.; Gray, H. B. *Inorg. Chem.* **1980**, *19*, 2462–2468.
(2) Sigal, I. S.; Gray, H. B. *J. Am. Chem. Soc.* **1981**, *103*, 2220–2225 and references therein.
(3) Smith, T. P. Ph.D. Thesis, California Institute of Technology, 1982.
(4) Bonati, F.; Malastesta, L. "Isocyanide Complexes of Metals"; Wiley: New York, 1969.
(5) Crociani, B.; Boschi, T.; Belluco, V. *Inorg. Chem.* **1970**, *9*, 2021–2025.
(6) Treichel, P. M.; Knesel, W. J.; Hess, R. W. *J. Am. Chem. Soc.* **1971**, *93*, 5424–5433.

0020-1669/84/1323-2572$01.50/0 